*Journal of Engineering Physics and Thermophysics, Vol. 79, No. 6, 2006*

# MATHEMATICAL SIMULATION OF THE PROCESS OF GROUP GROWTH OF CRYSTAL STRIPS FROM A MELT BY THE STEPANOV METHOD DEPENDING ON THE BEVEL ANGLE OF THE OPERATING SURFACE OF SHAPERS

**A. V. Zhdanov, S. N. Rossolenko, and V. A. Borodin**

UDC 536.421

*A mathematical model for determining the hydrodynamics of a melt and impurity concentration in the process of growing of a packet of sapphire strips by the Stepanov group method with beveled surfaces of shapers is considered. The description of the model contains: the Stefan problem, Navier–Stokes equation, diffusion equation, and Laplace capillary equation. The problems posed were solved numerically by the method of finite elements.*

The use of the Stepanov group method considerably increases the productivity of the process of group growth of crystal strips. At the same time, such a method of growing requires successful tuning of the thermal field in the thermal zone and an optimal configuration of shapers. Below, on the basis of a mathematical model, a group method of growing of sapphire strips for shapers with different bevel angles of their operating edges is considered. The work is a continuation of a previously published one [1], and is mainly devoted to determination of the hydrodynamics of a melt and impurity concentration in each strip of the packet depending on the bevel angle of the operating surfaces of shapers. Thus, in addition to the equations given in [1], the statement of the problem is supplemented by a diffusion equation. In many cases, the position and shape of the front are of importance. Here, a substantial influence can be exerted by the bevel angle. Therefore, in the work, investigation of the behavior of the crystallization front of grown strips is also carried out. The presence of radiation heat transfer between the side surfaces of the strips is assumed.

The aim of the finite-element analysis is the determination of the process parameters allowing one to minimize the following factors: 1) the difference in the distributions of temperature in a growing packet of strips to control the process by changing the heating power; 2) the impurity concentration at the crystallization front near the side surface.

The problem consists of a number of iteration procedures that ensure a constant growth angle and agreement between the temperatures of the side surfaces of plates and the densities of radiation fluxes between them.

**Statement of the Problem.** We will take into consideration the fact that the problem of heat conduction should be formulated separately for each inner strip and two outer ones. This follows from the difference in heat transfer between the side surfaces of the inner strips and the outer surfaces of the first and last strips and the environment.

The diagram of the crystallization process and selection of a coordinate system are presented in Fig. 1. Subscripts 1 and 2 at D correspond to the quantities relating to the melt and crystal, respectively. The temperature distribution in regions $D_1$ and $D_2$, which include the melt of the meniscus and crystal, is described by the heat-conduction equation

$$\Delta T_i - \zeta_i (V_i, \nabla T_i) = 0 , \quad (x, y) \cup D_i , \quad \zeta_i = \frac{\rho_i c_i}{k_i} , \quad i = 1, 2 , \tag{1}$$

where $V_1 = (u_1, v_1)$ is the field of velocities in the melt of the meniscus and $V_2 = (0, V_0)$ is the speed of pulling a crystal.

Institute of Solid-State Physics, Russian Academy of Sciences, Chernogolovka, Moscow Region, 142432, Russia; email: zhdan@issp.ac.ru. Translated from Inzhenerno-Fizicheskii Zhurnal, Vol. 79, No. 6, pp. 43–48, November–December, 2006. Original article submitted July 11, 2005; revision submitted April 28, 2006.

1062-0125/06/7906-1091 

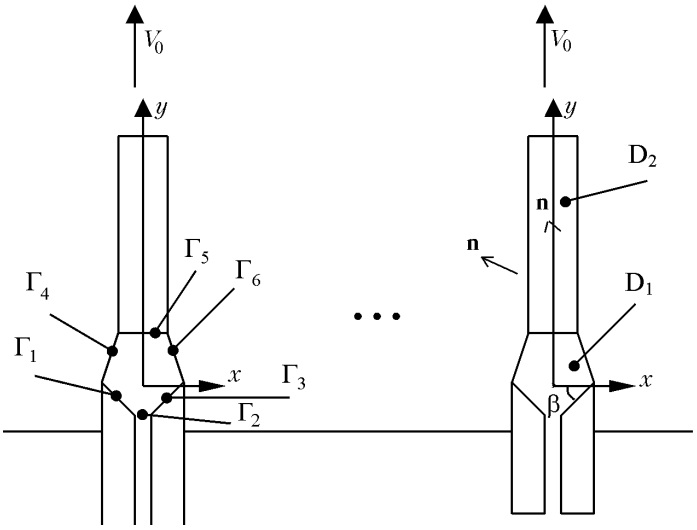


Fig. 1. General scheme of the group process of growing strips by the Stepanov method. Dots denote inner crystals.

At the interphase boundary $H(x)$, the Stefan condition and the condition of temperature continuity are to be satisfied:

$$k_2 (n, \nabla T_2) - k_1 (n, \nabla T_1) = \rho_2 V_0 \Delta H_f (1 + H_x'^2)^{1/2}, \tag{2}$$

$$T_1 [x, H(x)] = T_2 [x, H(x)] = T_m, \quad -h_1 \le x \le h_2, \quad y = H(x). \tag{3}$$

For the two side surfaces of the exterior strips, the heat transfer between the melt, crystal, and environment at temperature $T_{en}(y)$, which depends only on the height, is effected by convection and radiation:

$$-k_i \frac{\partial T_i}{\partial \mathbf{n}} = \eta_i (T_i - T_{en}) + \sigma \varepsilon_i (T_i^4 - T_{en}^4). \tag{4}$$

The equations that describe radiation heat transfer between the side surfaces of the inner strips will be defined below. On the operating surface of the shaper and at the end of the crystal the following temperatures are assigned:

$$T_1\Big|_{\Gamma_1} = T_f + \frac{x}{\cos\beta} (T_{en} - T_f), \quad T_2 (x, l) = T_2^0 (x), \quad -h_1 \le x \le h_2. \tag{5}$$

Temperature $T_1$ decreases linearly from $T_f$ to $T_{en}$ on $\Gamma_1$, it is constant on $\Gamma_2$, equal to $T_{en}$, and increases linearly from $T_{en}$ to $T_f$. The profile curve of the meniscus $f(y)$ satisfies the Laplace equation and boundary conditions:

$$\rho_2 g (y + H_{eff}) = \sigma_{liq,g} \frac{d}{dy}\left[\frac{df/dy}{(1 + (df/dy)^2)^{1/2}}\right], \tag{6}$$

$$f(0) = a, \quad -\frac{df}{dy}\Big|_{y=H(h_2)} = \tan\varepsilon_0. \tag{7}$$

The field of the distribution of velocities $V_1 = (u_1, v_1)$ in the melt satisfies the Navier–Stokes equation:

$$\mu \Delta V_1 + \rho_1 (V_1, \nabla) V_1 = \nabla P + F, \quad F = (0, -\rho_1 g), \tag{8}$$

$$\operatorname{div} V_1 = 0 . \tag{9}$$

Equation (9) allows one to introduce the stream function $\psi$ conventionally. The behavior of the melt flow will be described in what follows in terms of this function. The boundary of region $D_1$ consists of six parts ($\Gamma_i$, $i$ = 1, ..., 6) on which boundary conditions are assigned in conformity with the conditions of the melt flow. At the interphase boundary $y = H(x)$ for boundary $\Gamma_2$ we have

$$V_{1n} = V_0\left[1 + (H_x')^2\right]^{1/2}, \quad V_{1\tau} = 0 . \tag{10}$$

At boundaries $\Gamma_4$ and $\Gamma_6$, corresponding to the free surface of the melt, the normal velocity component is equal to zero:

$$V_{1n} = 0 , \quad [(\boldsymbol{\tau}, D^{\mathrm{t}}V_1), \mathbf{n}] = 0 , \quad x = f(y) . \tag{11}$$

At boundaries $\Gamma_1$, $\Gamma_3$, and $\Gamma_2$, which correspond to the operating surface of the shaper and capillary exit, the following conditions are satisfied:

$$u_1 = 0 , \quad v_1 = 0 , \quad (x, y) \cup \Gamma_1 \cup \Gamma_3 , \quad u_1 = 0 , \quad v_1 = AV_0\left[1 - \left(\frac{x}{d_0}\right)^2\right], \quad (x, y) \cup \Gamma_2 . \tag{12}$$

The constant $A$ entering into Eq. (12) is determined from the condition of equality of the melt fluxes through the capillary channel (boundary $\Gamma_2$) and through the crystallization front (boundary $\Gamma_5$):

$$A = \frac{3}{4d_0}\int_{-b}^{b}\left(1 + H'^2(x)\right)dx . \tag{13}$$

We assume that the side surfaces of all the strips are diffusely gray. This means that part of the radiation flux $q_{i,k}(r_k)$ is reflected by the side surface of the strip in all directions. The net radiation flux for the surface will be written as

$$q_k(r_k) = q_{0,k}(r_k) - q_{i,k}(r_k) , \quad k = 1, 2 , \tag{14}$$

where subscripts 1 and 2 denote the surfaces of the strips located opposite each other.

In the case of radiation heat transfer between two parallel, diffusely gray surfaces, the effective radiation flux $q_{0,k}(r_k)$ is the sum of the fluxes of self-radiation and reflected radiation, and it is described by the system of integral equations [2]

$$q_{0,k}(r_k) = \varepsilon_k\sigma T_k^4(r_k) + (1 - \varepsilon_k)\, q_{i,k}(r_k) , \tag{15}$$

$$q_{0,1}(y) - (1 - \varepsilon)\frac{1}{2}\int_0^L q_{0,2}(x)\frac{b^2}{[(x - y)^2 + b^2]^{3/2}}dx = \sigma\left(\varepsilon T_1^4(y) + (1 - \varepsilon)\, T_{\mathrm{r}}^4\right), \tag{16}$$

$$q_{0,2}(y) - (1 - \varepsilon)\frac{1}{2}\int_0^L q_{0,1}(x)\frac{b^2}{[(x - y)^2 + b^2]^{3/2}}dx = \sigma\left(\varepsilon T_2^4(y) + (1 - \varepsilon)\, T_{\mathrm{r}}^4\right), \tag{17}$$

where

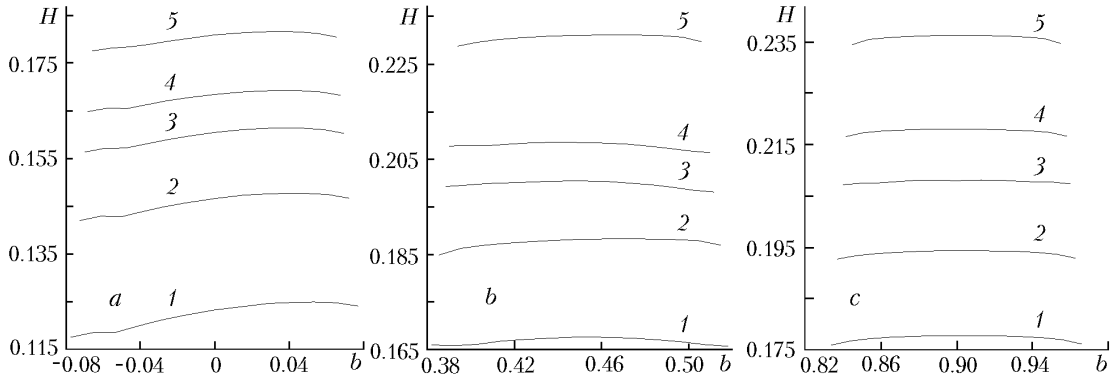


Fig. 2. Position and shape of crystallization fronts (a, b, and c for the first, second, and third crystals, respectively) at bevel angles of the operating edge of the shapers of: $60^{\circ}$ (1); $45^{\circ}$ (2); $30^{\circ}$ (3); $20^{\circ}$ (4); $5^{\circ}$ (5).

$$T_{\mathrm{r}}^4 = T_{\mathrm{s}}^4 \frac{1}{2}\left[1 - \frac{y}{\sqrt{y^2 + b^2}}\right]; \quad b = d + 2a - h_1^{(2)} - h_2^{(1)}.$$

By solving this system of equations, we find the values of $q_{0,1}$ and $q_{0,2}$ and then find the distributions of the fluxes of net radiations $q_1$ and $q_2$:

$$q_k(y) = \frac{\varepsilon}{1-\varepsilon}\left(\sigma T_k^4(y) - q_{0,k}(y)\right), \tag{18}$$

whereas, when using the incident fluxes $q_{i,k}$, we obtain

$$q_k(y) = \varepsilon\left(\sigma T_k^4(y) - q_{i,k}(y)\right) = \varepsilon\sigma\left(\sigma T_k^4 - T_{\mathrm{en}k}^4\right), \tag{19}$$

where

$$T_{\mathrm{en}k} = \sqrt[4]{q_{i,k}/\sigma}, \quad k = 1, 2, \tag{20}$$

i.e., we obtain a radiation law similar to (4), only with other temperatures of surrounding media $T_{\mathrm{en}k}$. Thus, for the inner strips the heat-transfer law will be presented in the form of expression (4) if we assume that $T_{\mathrm{en}} = T_{\mathrm{en}k}$.

The distribution of the impurity concentration in the melt is described by the equation

$$\mathring{D}\,\Delta C - \mathbf{V}\nabla C = 0 \tag{21}$$

and boundary conditions

$$\frac{\partial C}{\partial y} = 0, \quad (x, y) \cup \Gamma_1 \cup \Gamma_3, \quad C = C_0, \quad (x, y) \cup \Gamma_2, \quad \frac{\partial C}{\partial \mathbf{n}} = 0, \quad (x, y) \cup \Gamma_4 \cup \Gamma_6,$$

$$-\mathring{D}\,\frac{\partial C}{\partial \mathbf{n}} = V_0(k_0 - 1)\,C, \quad (x, y) \cup \Gamma_5.$$

The solution of the problem in the given formulation by the method of finite elements is given in [3–5].

**Results of Numerical Analysis.** Numerical calculations showed that the bevel angle of the operating surface of a shaper substantially influences such characteristics of growth as the shape and position of the crystallization front, the hydrodynamics of the melt, and distribution of impurity concentrations in the melt meniscus.

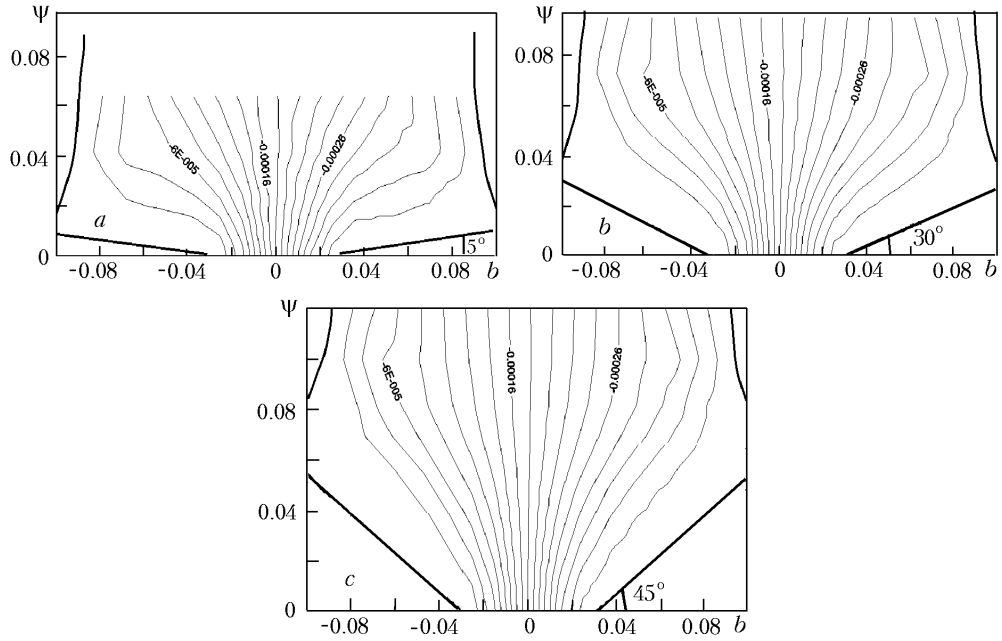


Fig. 3. Hydrodynamics of the melt.

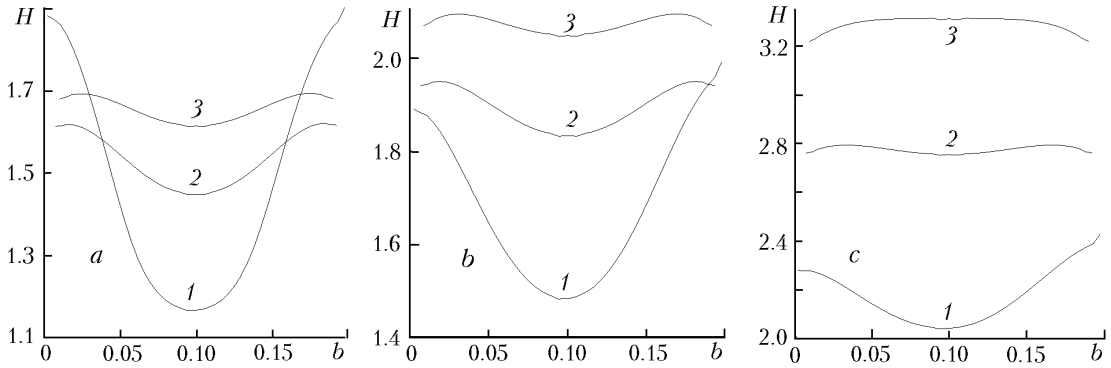


Fig. 4. Concentrations of impurities at the crystallization front (bevel angles of the operating edge of shapers: a) $5^{o}$; b) $30^{o}$; c) $45^{o}$); 1) first crystal; 2) second crystal; 3) third crystal.

We considered a packet consisting of six strips ($N$ = 6), with a distance between the shapers of 0.25 cm for bevel angles $5^{o}$, $20^{o}$, $30^{o}$, $45^{o}$, and $60^{o}$. The crystallization fronts obtained are shown in Fig. 2, from which it is seen that with increase in the bevel angle the crystallization front descends approximately from 0.18 to 0.12 mm on the first (exterior) strip and from 0.235 to 0.175 mm on the second and third strips. It should be noted that in all strips of the packet the difference in the shape of the front from a plane one is most evident at larger angles.

Next, we investigated the case where the distance between the first and second strips was 1 cm, with the remaining distances being equal as before to 0.25 cm. As a result, a decrease in the height of the menisci in all of the internal crystals was noted: on average by about 0.05 mm and by 0.1 mm on the first and last strips. No appreciable changes in the shape of the front were noticed.

The bevel angle of the operating edge of a shaper appreciably influences the hydrodynamics of the melt. Indeed, with increase in the bevel angle the region of melt flow becomes larger. The jet flow escaping from the capillary near the crystallization front can be not so appreciable if the bevel angle is large enough. Figure 3 vividly demonstrates that the flow becomes more uniform in the region located far from the capillary exit, which, of course, must influence the behavior of the impurity concentration.

Especially important is the behavior of the impurity at the crystallization front, since precisely this determines its role in the crystal (Fig. 4). The impurity is distributed most nonuniformly in the first crystal. The second and third crystals are rather close in the character of impurity behavior, and the values of the impurity concentration along the crystallization front increase substantially with the bevel angle. In the central crystals, at a large bevel angle, the values of the impurity concentration at the center of the crystals may be higher than on the edges. This behavior of concentrations is explained by the different height of the menisci of the melt and by the hydrodynamics of the latter.

Thus, we have considered a mathematical model for calculating the distributions of temperature and concentrations of impurity in the process of growing sapphire strips by the Stepanov group method depending on the bevel angle of the operating surfaces of shapers. Based on mathematical simulation, different values of technological parameters have been analyzed to optimize the process of growing. It has been established that reduction of the distance between shapers leads to a decrease in the difference between the temperature distributions in the strips. It can also be decreased by using shields that emulsify the exterior strips. The temperature of the operating surfaces of shapers must not decrease to avoid a sharp increase in the impurity concentrations. The decrease in the temperature can be controlled by observing the height of the meniscus of measuring the signal from the crystal weight sensor. An increase in the bevel angle of the operating surfaces of the shapers leads to a decrease in the height of the meniscus and, consequently, to a greater stability of the process of growth.

## NOTATION

a, half-thickness of a shaper, mm; $A$, constant determined from the condition of equality of the melt flows through the capillary channel and crystallization front; $b$, half-thickness of crystalline strips, mm; $c$, heat capacity; J/K; $C$, impurity concentration, $\text{mm}^{-3}$; $d$, distance between adjacent shapers, mm; $d_0$, half-thickness of the capillary channel, mm; $D$, computational domain; $\mathring{D}$, diffusion coefficient, $\text{m}^{-2}$; $D^{\text{t}}$, deformation tensor; $f$, profile curve of the meniscus, m; $F$, external specific force, $\text{N/m}^3$; $g$, free fall acceleration, $\text{m/sec}^2$; $H$, curve of crystallization front, m; $H_{\text{eff}}$, distance between the melt surface and the meniscus base line, mm; $h_2^{(1)}$ and $h_1^{(2)}$, values reckoned from the $y$ axis to the side adjacent surfaces of neighboring strips; $k_i$, thermal conductivity coefficient, J/(K·m·sec); $k_0$, coefficient of impurity distribution; $l$, running length of crystals, m; $L$, length of the packet strips, mm; $N$, number of strips in a packet; $\mathbf{n}$, unit normal vector to the boundary of the computational domain, m; $P$, outer pressure, Pa; $q$, radiation flux, $\text{J/(m}^2\cdot\text{sec)}$; $T$, temperature, K; $T_{\text{r}}$, temperature expressed in terms of $T_{\text{s}}$, K; $T_{\text{s}}$, known temperature of the surface of the common base between two neighboring shapers, K; $u_1$, component of the melt-velocity normal to the boundary, m/sec; $v$, melt-velocity component tangent to the boundary, m/sec; $V_0$, speed of pulling of crystals, m/sec; $\beta$, bevel angle of shapers, deg; $\Gamma$, boundary of the region; $\Delta H_{\text{f}}$, specific heat of crystallization, J/kg; $\varepsilon_i$, emissivity; $\varepsilon_0$, growth angle, deg; $\zeta$, heat-transfer coefficient, $\text{W/(m}^2\cdot\text{K)}$; $\eta_i$, heat-conduction coefficient, $\text{J/(K·m}^2\cdot\text{sec)}$; $\mu$, dynamic viscosity of the melt, Pa·sec; $\rho_i$, density, $\text{kg/m}^3$; $\sigma$, Stefan–Boltzmann constant, $\text{W/(m}^2\cdot\text{K}^4\text{)}$; $\sigma_{\text{liq,g}}$, coefficient of surface tension of the melt, $\text{J/m}^2$; $\boldsymbol{\tau}$, unit tangent vector to the profiled curve of the meniscus, m; $\psi$, stream function of the melt. Subscripts: en, environment; eff, effective quantity; f, shaper surface; $i$, melt (1) or crystal (2); $k$, surfaces of neighboring strips; liq,g, value in transition from a liquid to a gaseous medium; m, melting; r, shaper (radiative); s, common base between shapers; t, tensor.

## REFERENCES


1. A. V. Borodin, A. V. Zhdanov, L. P. Nikolaeva, I. S. Pet'kov, and L. P. Chupyatova, Temperature stresses in a packet of strips produced from a melt by the Stepanov method, *Inzh.-Fiz. Zh.*, **74**, No. 3, 106–112 (2001).
2. G. Strang and G. J. Fix, *An Analysis of the Finite Element Method*, Prentice-Hall, Englewood Cliffs (1973).
3. R. Siegel and J. R. Howell, *Thermal Radiation Heat Transfer* [Russian translation], Mir, Moscow (1975).
4. C. A. J. Fletcher, *Computational Galerkin Methods*, Springer, New York–Berlin–Heidelberg–Tokyo (1984).
5. A. R. Mitchell and R. Wait, *The Finite Element Method in Partial Differential Equations* [Russian translation], Mir, Moscow (1981).